Chinese Chemical Letters 32 (2021) 1819–1822

Contents lists available at ScienceDirect

Chinese Chemical Letters

journal homepage: www.elsevier.com/locate/cclet

Communication

Zn-based metal organic framework derivative with uniform metal sites and hierarchical pores for efficient adsorption of formaldehyde

Junjie Yang[a], Junxian Qin[a], Ziyang Guo[a], Yun Hu[a,b,c,*], Xia Zhang[d]

[a] School of Environment and Energy, South China University of Technology, Guangzhou 510006, China
[b] Guangdong Provincial Key Laboratory of Atmospheric Environment and Pollution Control, Guangzhou 510006, China
[c] The Key Lab of Pollution Control and Ecosystem Restoration in Industry Clusters, Ministry of Education, Guangzhou 510006, China
[d] Zhejiang Tianchuan Environmental Science& Technology Co., Ltd., Hangzhou 310015, China

ARTICLE INFO

Article history:
Received 15 August 2020
Received in revised form 10 October 2020
Accepted 17 November 2020
Available online 20 November 2020

Keywords:
Formaldehyde
Adsorption
Hierarchical Pore
MOF-derivative
Carbon

ABSTRACT

A Zn-containing graphite carbon (Zn-GC) with uniform Zn metal sites and hierarchical pore structure was obtained by pyrolysis of Zn-based metal organic framework (MOF). Zn-GC exhibited excellent adsorption capacity and reproducibility for formaldehyde. The adsorption capacity of Zn-GC was 736 times that of commercial activated carbon and 5.6 times that of ZSM-5 adsorbents. The characterization and experimental results showed that the surface chemical characteristics of the adsorption material play an important role in the adsorption performance. The superior performance was attributed to Zn metal sites and oxygen-containing functional groups on the MOF derivative as well as hierarchical pore structure. The material showed a great potential in the field of organic pollutant removal.

Formaldehyde is a volatile organic compound (VOC) with irritating odor, which is widely present in daily life and industrial production [1–3]. Long-term exposure of the human body to formaldehyde can cause damage to health. Therefore, formaldehyde has been attracted great attention and identified as Class I carcinogen by the World Health Organization. There are many methods for formaldehyde removal, such as adsorption, photocatalysis and combustion. So far, the adsorption is the most widely used method [4–10]. However, the commonly used adsorption materials (such as activated carbon and zeolite) suffered from rapid deactivation in practical application due to the short life, low adsorption efficiency and poor moisture resistance.

In recent years, metal organic frameworks (MOFs) have been regarded as the ideal adsorption materials due to the uniform distribution of pores and metal active sites [11–13]. Nonetheless, because of the unstable organic structure and the existence of only micropores, the adsorption performance of MOFs in practical use is limited, and the structure is easy to collapse [14]. In order to overcome these disadvantages, the derivatives of MOFs have recently received more and more attention owing to its stable structure [15–17]. However, the adsorption of VOCs by MOF derivatives has been rarely reported, and the roles of metal sites and carbon framework in the adsorption need to be further studied.

In this work, by using a MOFs material ZIF-8 as the precursor of derivative, a graphite carbon material (Zn-GC) with hierarchical pore structure and Zn active sites was synthesized. The material exhibited excellent activity, high stability and renewability in the adsorption of formaldehyde. To investigate the role of each part of Zn-GC in the process of formaldehyde adsorption, conditional experiments and the characterization of the adsorbent surface structure were carried out and discussed.

The adsorbent Zn-GC was synthesized by the pyrolysis of ZIF-8 [18]. 2-Methylimidazole and $Zn(NO_3)_2{\cdot}6H_2O$ were respectively dissolved in 50 mL methanol solution, then mixed and stirred for 24 h to obtain ZIF-8. The X-ray diffraction (XRD) pattern of ZIF-8 was shown in Fig. S1 (Supporting information). After washing and drying, ZIF-8 was calcined under an N_2 atmosphere in a series of temperatures to obtain Zn-GC-X, where the X = 550, 650, 750 and 850 °C. The scanning electron microscope (SEM) measurement (Figs. 1a and b) showed that the structure and size of Zn-GC were similar to that of the precursor ZIF-8, the particle size of rhombic dodecahedron structure was about 200 nm. The energy dispersive spectrum (EDS) mapping analysis showed that Zn was uniformly distributed on the surface of the material (Fig. S2 in Supporting information).

* Corresponding author at: School of Environment and Energy, South China University of Technology, Guangzhou 510006, China.
E-mail address: huyun@scut.edu.cn (Y. Hu).

https://doi.org/10.1016/j.cclet.2020.11.023
1001-8417/

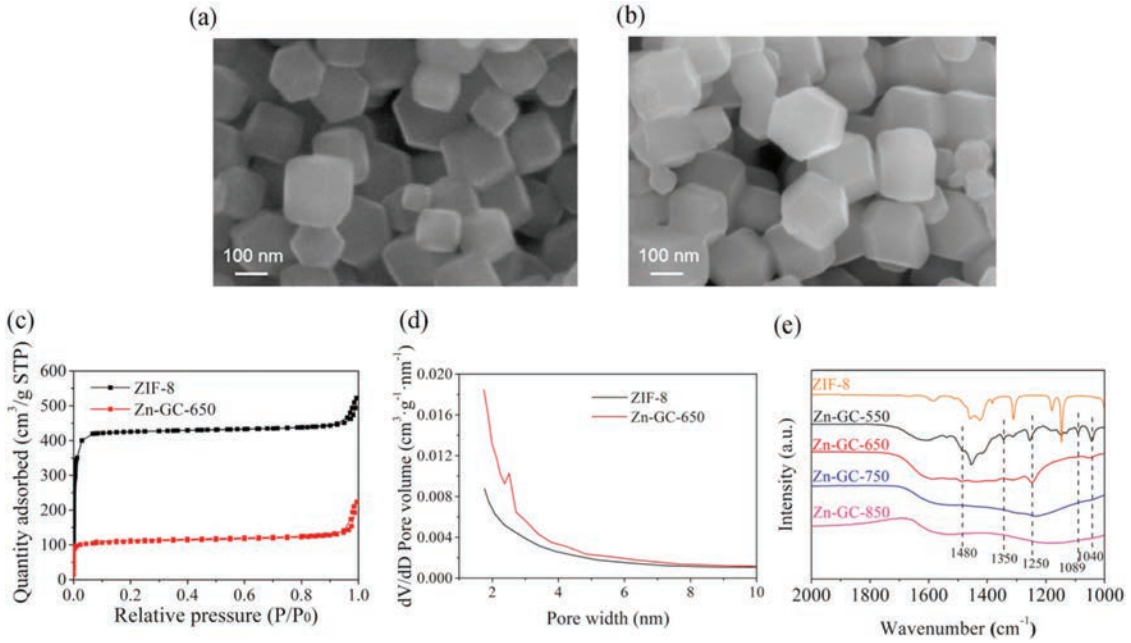

Fig. 1. SEM image of (a) ZIF-8, (b) Zn-GC-650. (c) N_2 adsorption–desorption isotherms. (d) The aperture distribution patterns of ZIF-8 and Zn-GC-650. (e) FTIR spectra of ZIF-8 and Zn-GC calcined at different temperature.

From the N_2 adsorption–desorption isotherms (Fig. 1c) and the analysis of pore structure (Table S1 in Supporting information), the specific surface area of Zn-GC was smaller than that of ZIF-8. The original pore structure collapsed to a certain extent, so the surface aera decreased. But as the calcining temperature raised, the average pore size getting larger and the surface aera began to increase due to the forming of porous carbon. It can be seen from the aperture distribution patterns that Zn-GC formed the hierarchical pore structure including micropores and mesopores (Fig. 1d). Combined with the SEM characterization, the obtained Zn-GC inherited the original channel and the active Zn sites of ZIF-8. The Fourier transform infrared spectrometer (FTIR) results of ZIF-8 and the calcined samples are shown in Fig. 1e. On ZIF-8, the imidazole ring vibration signal was found at 1300−1500 cm^{-1} and the peak at about 1583 cm^{-1} could be assigned to the C=N stretch mode. As the temperature raised to 550 °C, the characteristic peaks of C—OH appeared at 1040, 1089 and 1250 cm^{-1}, the peaks of −CHO occurred at about 1350 and 1480 cm^{-1} [19,20]. When further heated up to 650 °C, the signals of the imidazole ring and most of functional groups disappeared, only the C—OH signal existed at 1250 cm^{-1}, which indicated that the imidazole skeleton was converted to graphite carbon. When the calcining temperature increased to 750 °C, the signals of surface functional groups disappeared. As the temperature raised to 850 °C, the spectrum was smoother and no significant peak was found, which indicated a higher degree of graphitization.

To investigate the adsorption capacity of Zn-GC and the role of surface functional groups, the formaldehyde adsorption for Zn-GC samples calcined at different temperatures were tested through a dynamic adsorption device (Fig. S3 in Supporting information). 0.1 g of dried Zn-GC was mixed with 0.2 g of quartz sand in the test, the relative humidity was adjusted to 0 to avoid the impact of water and the concentration of formaldehyde was 10 ppm. The concentration of formaldehyde was detected by a formaldehyde detector (the details can be seen in Supporting information). As shown in Fig. 2a, although ZIF-8 had a larger surface area, the adsorption performance was very poor, the breakthrough adsorption capacity was only 0.44 mg/g, which can be attributed to the size limitation of the micropore structure. The formaldehyde adsorption capacity of calcined samples was significantly increased compared with ZIF-8. The breakthrough adsorption capacities of Zn-GC-550, Zn-GC-650, Zn-GC-750 and Zn-GC-850 were 16.67, 17.57, 13.49 and 11.32 mg/g, respectively, among which Zn-GC-650 exhibited the best performance. In the FTIR pattern (Fig. 1e), Zn-GC-550 still had a strong signal at 1300−1500 cm^{-1}, it indicated that Zn-GC-550 also contained imidazole structure and was accordance with the pore size result in Table S1, which was similar with its precursor ZIF-8. The formaldehyde adsorption of

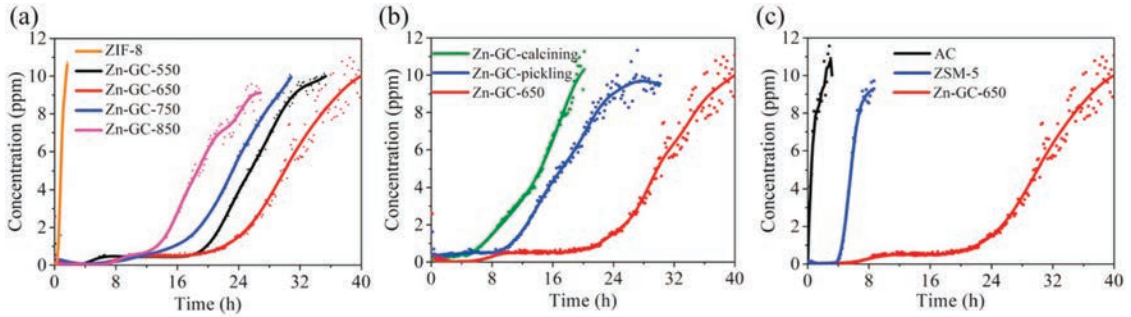

Fig. 2. Formaldehyde adsorption performance of (a) ZIF-8 and Zn-GC calcined at different temperatures, (b) before and after Zn removal, (c) Zn-GC-650 and commercial materials.

Table 1
The formaldehyde adsorption capacities of the samples with different Zn contents.

Sample	Mass% of Zn	Adsorption capacity (mg/g)
Zn-GC-650	12.84	17.57
Zn-GC-pickling	4.67	9.64
Zn-GC-calcining	1.75	6.06

Zn-GC-550 was lower than that of Zn-GC-650 also mainly due to the size limitation. On the other side, with the increase of calcining temperature, although the surface aera increased, the pore size of the Zn-GC-750 and Zn-GC-850 were too large to capture the formaldehyde (Table S1) [2]. And the oxygen-containing functional groups on the surface of the Zn-GC decreased (Fig. 1e). It is generally accepted that oxygen-containing functional groups can interact with VOCs by combining the hydrogen bonds [10]. The decrease of oxygen-containing groups resulted in the reduction of the formaldehyde affinity, thus decreasing the adsorption capacities of Zn-GC-750 and Zn-GC-850.

To study the impact of metal sites to the formaldehyde adsorption process, Zn in the material was removed by two methods respectively: Pickling in 2 mol/L HCl (GC-pickling) or high temperature calcination at 950 °C (GC-calcining), which had been widely used to remove the Zn metal [18,21] (the details can be seen in Supporting information). According to the SEM and EDS analyses, most of the Zn were removed and the samples maintained the morphology (Figs. S4-S8 in Supporting information). The adsorption capacity of both Zn-GC-pickling and Zn-GC-calcining significantly decreased. It was worth noting that lower Zn content had lower adsorption performance (Fig. 2b, Table 1), the adsorption capacity of Zn-GC-pickling was reduced to 9.24 mg/g while that of Zn-GC-calcining was only 6.06 mg/g, which indicated that the Zn metal sites had a strong affinity for formaldehyde.

The formaldehyde adsorption performance of Zn-GC-650 with commercial adsorbents was also compared. The adsorption capacity of Zn-GC-650 was significantly superior to that of commercial ZSM-5 and activated carbon (Fig. 2c). The adsorption capacity of Zn-GC-650 was 17.57 mg/g, which was 763 times that of commercial activated carbon (0.023 mg/g) and 5.6 times that of ZSM-5 (3.14 mg/g). This may be owing to the uniform distributed metal adsorption sites and oxygen containing functional groups, which made Zn-GC had a stronger affinity to formaldehyde. This result indicated that Zn-GC has a promising application prospect in formaldehyde removal.

The moisture resistance is a key factor for the high-performance adsorbent, high humidity would cause the blocking of the material pores or the collapse of structure [22]. The formaldehyde adsorption experiment was carried out under the 90% of relative humidity. The adsorption efficiency of Zn-GC under the high humidity environment maintained above 99% for at least 56 h (Fig. 3a), which was much higher than that of Zn-GC under low humidity. This could be attributed to the hierarchical pore structure, which is able to hold water in the channels to prevent the pore structure from blocking [23,24]. At the same time, the adsorbed water on the surface of the material formed the hydrogen bond with formaldehyde molecules, which further enhanced the adsorption effect of formaldehyde [25,26]. However, the adsorption capacity of ZSM-5 with microporous structure decreased under the condition of high humidity (Fig. 3b). This may be due to the water vapor blocking part of the channel and the limitation of pore size, making it impossible for formaldehyde molecules bound to water to pass through [27–30]. This further exhibited the advantages of the hierarchical structure for formaldehyde adsorption in the high humidity environments. The results also showed that the prepared material has a potential application value for the removal of pollutants in complex environment.

The renewability of the Zn-GC adsorbent was examined as the economic efficiency is important for the practical application. The adsorbed formaldehyde on Zn-GC-650 was detached under the heating in N_2 flow, and no apparent changes were observed in SEM images after the regeneration (Fig. S9 in Supporting information). Then the refresh Zn-GC-650 was used again for formaldehyde adsorption. The activity remained unchanged (Fig. 3c), indicating that the Zn-GC structure was stable. Comparing the FTIR spectra before and after the adsorption, the characteristic peaks of adsorbed aldehyde species occurred at 1600 and 1668 cm^{-1} (Fig. 3d) [31,32]. The other characteristic peaks were the same, suggesting that no significant changes occurred on the surface of Zn-GC during the adsorption process.

Based on the above results, a mechanism to explain the outstanding performance of Zn-GC for formaldehyde adsorption can be proposed (Fig. 3e). First of all, the oxygen containing functional groups and metal sites on the surface of the carbon-based MOF derivative had a strong affinity for polar formaldehyde

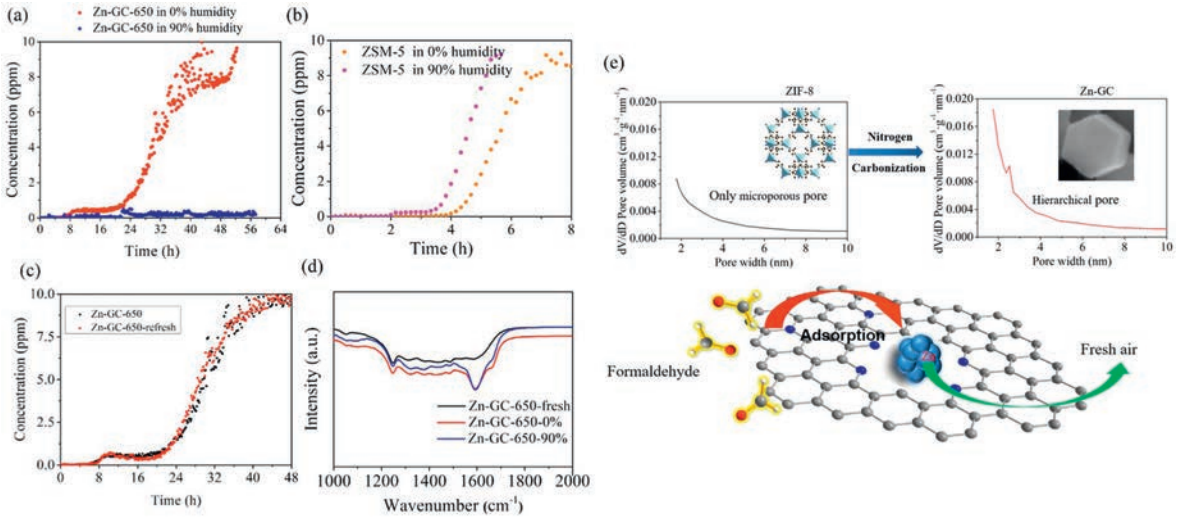

Fig. 3. The adsorption performance of (a) Zn-GC-650 and (b) ZSM-5 under different humidities, (c) the performance of Zn-GC-650 and Zn-GC-650-refresh. (d) The FT-IR pattern before and after the adsorption; (e) Proposed mechanism of formaldehyde adsorption on GC-N-Zn.

molecules, which was conducive to the adsorption of formaldehyde. Secondly, the carbon-based MOF derivative had stable chemical properties, which avoided the collapse of the structure during the adsorption process, and also made it have a good reproducibility. Finally, the hierarchical porous structure of the framework, which provided enough space to pass through and hold the water vapor in the air, was avail to the mass transfer, thereby enhancing the capture of formaldehyde through hydrogen bonding.

In this work, a graphite carbon material with Zn site (Zn-GC) was synthesized. The results demonstrated that Zn-GC had superior adsorption and regeneration performance compared with commercial adsorbents. These excellent properties were attributed to the Zn metal sites and oxygen-containing functional groups on the MOF derivative as well as the hierarchical pore structure. This study revealed the reason for MOF derivatives with excellent formaldehyde adsorption capacity and provided new insights for the application of MOF derivatives as VOC adsorption materials.

Declaration of competing interest

The authors report no declarations of interest.

Acknowledgments

This work was supported by The National Key Research and Development Program of China (No. 2018YFB0605200), Scientific Research Project of Guangzhou City (No. 201804020026), National Natural Science Foundation of China (No. 21777047) and National Training Program of Innovation and Entrepreneurship for Undergraduates (No. S201910561224).

Appendix A. Supplementary data

Supplementary material related to this article can be found, in the online version, at doi:https://doi.org/10.1016/j.cclet.2020.11.023.

References

[1] N. Aldag, J. Gunschera, T. Salthammer, Cellulose 24 (2017) 4509–4518.
[2] C.J. Na, M.J. Yoo, D.C. Tsang, et al., J. Hazard. Mater. 366 (2019) 452–465.
[3] C. He, J. Cheng, X. Zhang, et al., Chem. Rev. 119 (2019) 4471–4568.
[4] L.L. Zhu, D.K. Shen, K.H. Luo, J. Hazard. Mater. 389 (2020) 122102.
[5] Y. Lv, J. Sun, G.Q. Yu, et al., Microporous Mesoporous Mater. 294 (2019) 109869.
[6] K.J. Kim, H.G. Ahn, Carbon 48 (2010) 2198–2202.
[7] H.L. Chiang, P.C. Chiang, C.P. Huang, Chemosphere 47 (2002) 267–275.
[8] S.S. Huang, W. Deng, L. Zhang, et al., Microporous Mesoporous Mater. 302 (2020) 110204.
[9] Y. Wang, K. Liu, J. Wu, et al., ACS Catal. 10 (2020) 10021–10031.
[10] X.Q. Li, L. Zhang, Z.Q. Yang, et al., Sep. Purif. Technol. 235 (2020) 116213.
[11] Q.Q. Huang, Y. Hu, Y. Pei, J.H. Zhang, M.L. Fu, Appl. Catal. B 259 (2019) 118106.
[12] J.H. Zhang, Y. Hu, J.X. Qin, Z.X. Yang, M.L. Fu, Chem. Eng. J. 385 (2020) 123814.
[13] X. Guan, Y. Wang, W.F. Cai, Chin. Chem. Lett. 30 (2019) 1310–1314.
[14] X.M. Zheng, S. Liu, S. Rehman, Z.H. Li, P.Y. Zhang, Chem. Eng. J. 389 (2020) 123424.
[15] N. Zhang, L.M. Yan, Y. Lu, et al., Chin. Chem. Lett. 31 (2020) 2071–2076.
[16] S. Jafari, F. Ghorbani-Shahna, A. Bahrami, H. Kazemian, Microporous Mesoporous Mater. 268 (2018) 58–68.
[17] F.C. Chu, Y. Zheng, B.Y. Wen, et al., RSC Adv. 8 (2018) 2426–2432.
[18] J.X. Qin, J. Wang, J.J. Yang, et al., Appl. Catal. B 267 (2020) 118667.
[19] L.C. Chen, W. Cui, J.Y. Li, et al., Appl. Catal. B 271 (2020) 118948.
[20] Y. Hu, H. Kazemian, S. Rohani, Y.N. Huang, Y. Song, Chem. Commun. 47 (2011) 12694–12696.
[21] S. Xue, Y.J. Yu, S.S. Wei, et al., J. Taiwan Inst. Chem. Eng. 91 (2018) 539–547.
[22] Y.S. Luo, B.Q. Tan, X.H. Liang, et al., Microporous Mesoporous Mater. 297 (2020) 110034.
[23] J. Miao, X.J. Zhao, Y.T. Li, Z.H. Liu, Colloids Surf. A 602 (2020) 124883.
[24] Y.L. Zhang, G.Z. Ji, C.J. Li, X.X. Wang, A.M. Li, Chem. Eng. J. 390 (2020) 124398.
[25] J.J. Wang, P.Y. Zhang, J. Li, et al., Environ. Sci. Technol. 49 (2015) 12372–12379.
[26] J. Rodriguez-Mirasol, J. Bedia, T. Cordero, J.J. Rodríguez, Sep. Sci. Technol. 40 (2005) 3113–3135.
[27] M. Thommes, K. Kaneko, A.V. Neimark, et al., Pure Appl. Chem. 87 (2016) 25-25.
[28] X. Chen, X. Jiang, C.J. Yin, B.L. Zhang, Q.Y. Zhang, J. Hazard. Mater. 367 (2019) 194–204.
[29] L. Feng, S. Yuan, L.L. Zhang, et al., J. Am. Chem. Soc. 140 (2018) 2363–2372.
[30] I.I. Laskar, Z. Hashisho, J.H. Phillips, J.E. Anderson, M. Nichols, Environ. Sci. Technol. 53 (2019) 2647–2659.
[31] M.T. Drexler, M.D. Amiridis, J. Catal. 214 (2003) 136–145.
[32] A.J. Van Hengstum, J. Pranger, S.M. Van Hengstum-Nijhuis, J.G. Van Ommen, P.J. Gellincs, J. Catal. 101 (1986) 323–330.